INL/CON-10-18053
PREPRINT

Fast-Neutron Spectrometry Using a ^{3}He Ionization Chamber and Digital Pulse Shape Analysis

2010 Symposium on Radiation Measurements and Applications

D. L. Chichester
J. T. Johnson
E. H. Seabury

May 2010

The INL is a
U.S. Department of Energy
National Laboratory
operated by
Battelle Energy Alliance

Fast-Neutron Spectrometry Using A ^{3}He Ionization Chamber and Digital Pulse Shape Analysis

D. L. Chichester*, J. T. Johnson, and E. H. Seabury

Idaho National Laboratory, 2525 N. Fremont Avenue, Idaho Falls, Idaho 83415

Abstract

Digital pulse shape analysis (dPSA) has been used with a Cuttler-Shalev type ^{3}He ionization chamber to measure the fast-neutron spectra of a deuterium-deuterium electronic neutron generator, a bare ^{252}Cf spontaneous fission neutron source, and of the transmitted fast neutron spectra of a ^{252}Cf source attenuated by water, graphite, liquid nitrogen, and magnesium. Rise-time dPSA has been employed using the common approach for analyzing n +^{3}He → ^{1}H + ^{3}H ionization events and improved to account for wall-effect and pile-up events, increasing the fidelity of these measurements. Simulations have been performed of the different experimental arrangements and compared with the measurements, demonstrating general agreement between the dPSA-processed fast-neutron spectra and predictions. The fast neutron resonance features of the attenuation cross sections of the attenuating materials are clearly visible within the resolution limits of the electronics used for the measurements, and the potential applications of high-resolution fast-neutron spectrometry for nuclear nonproliferation and safeguards measurements are discussed.

Keywords:

Neutron Spectrometry

Neutron Scattering

Californium-252

Helium-3 Ionization Counter

* Corresponding Author: Phone: (208) 526-8920 and Email: david.chichester@inl.gov

1 Introduction

One method to determine the energy distribution of a fast neutron radiation field is to use a ^{3}He ionization chamber and measure the amplitude of signal pulses from the device. In these detectors neutrons are absorbed by ^{3}He in the ^{3}He(n,p)^{3}H reaction, the resulting proton and tritium atom then proceed to ionize the gas in the ionization chamber and an electronic signal is registered as these electrons and ions are collected. Neutron capture in ^{3}He is exothermic with a Q-value of 0.764 MeV; the amplitude of signal pulses resulting from neutron capture corresponds to the sum of this Q value plus the incident neutron's energy. If proper care is taken to eliminate spurious noise signals and to amplify the small current pulses without adding noise, then a neutron energy resolution of better then 20 keV can be achieved. Specialized ^{3}He ionization chamber designs have been developed to achieve this level of performance and are described in the literature.[1-5] These instruments are occasionally referred to as Cuttler-Shalev (C-S) spectrometers after two early researchers in the field. More sophisticated detectors have been designed that incorporate ^{3}He between opposing surface barrier detectors, using solid-state electronics to record the coincident energy deposition from protons and tritium atoms directly, but they are generally limited to small sizes. [6,7]

Due to the presence of thermal neutrons in nearly all neutron measurement scenarios, energy spectra from ^{3}He spectrometers contain a peak in the energy distribution corresponding to the Q value itself; this is often referred to as the epithermal peak. Unfortunately, an interference resulting from neutron elastic scattering off of ^{3}He yields a continuum energy distribution in the spectrum at energies below ¾ E_n, for En ≥ 1.019 MeV this continuum begins to extend above the energy of the epithermal peak.[8] Neutron recoil off of other gases in the spectrometer, dense gases included to reduce the ionized particle path length, introduces a second type of background artifact in these instruments. At even higher energies additional interferences also become important including wall-effect artifacts from the incomplete deposition of energy when the proton and tritium atom ranges exceed the dimensions of the detector. A second peak occurs for higher energy neutrons due to the opening of the endothermic $^{3}He + n \rightarrow {}^{2}H + {}^{2}H$ reaction with a Q-value of -3.27 MeV.[9]

Pulse shape analysis may be used to eliminate many of these unwanted spectral artifacts; the techniques to achieve this are well known and have been reported in the literature cited above. These techniques exploit the fact that neutron capture events result in two charged particles traveling in the ionization counter's gas, a proton and a relatively heavier/slower/shorter-range tritium atom, while recoil events produce only one energetic helium atom.

Along the path of the charged particles in the spectrometer ion pairs are formed in the detector gas, which is often a mixture of ^{3}He and a heavier gas such as methane to shorten the particle path lengths. If the proton-tritium path or recoiling helium path are parallel to the detector's anode wire then the rise-time of the charge pulse is the same for both neutron capture events and neutron recoil events. However, if the path of these particles is skewed with respect to the anode, the longer path length of protons in the gas means it takes slightly more time for the total deposited energy of a proton-tritium pair to reach the anode then it does for a recoiling helium atom of the same energy.[10-12] The relation between the rise-time of the charge pulse and the pulse energy or amplitude is non-linear with respect to the deposited energy. However, with careful selection of a rejection criteria nearly all non-capture artifacts in the spectra of a ^{3}He ionization chamber may be rejected while only sacrificing on the order of ½ of the capture neutron pulses. Historically, this analysis has been done using analog electronics but some prior work has been demonstrated using digital pulse shape analysis (dPSA).[13]

The high-resolution neutron spectrometry capable when using C-S fast-neutron spectrometers is particularly useful when time-of-flight measurements cannot be conducted; C-S-type instruments have been used for many different applications. In the realm of nuclear physics C-S detectors have been used to measure delayed neutron spectra from fission products, to evaluate nuclear energy levels following charged particle nuclear reactions, and to study neutron spectra from fusion.[14-20] They have also been used to quantify the neutron spectra from radioisotope neutron sources and to evaluate neutron radiation fields for health physics applications.[7,21-23] The best method to evaluate the performance of a neutron spectrometer is to use a charged-particle accelerator to produce calibrated monoenergetic neutron fields of known energy and known intensity across a wide range of energies; an alternate approach is to use the ^{252}Cf transmission technique to make relative analyses of the performance of a C-S neutron spectrometer.[24]

Recently a research program at Idaho National Laboratory (INL) has started to evaluate fast-neutron spectrometry for nuclear nonproliferation, nuclear safeguards, and national security applications. Included in this work have been studies to evaluate the performance of ^{3}He-based neutron detectors for fast-neutron spectrometry. Without a variable energy monoenergetic neutron source at INL we have chosen to use the ^{252}Cf transmission technique to carry out this work, in conjunction with the use of dPSA waveform discrimination techniques. In this paper we report on work to evaluate a C-S style neutron spectrometer and to measure the transmission spectrum of a ^{252}Cf neutron source through several different materials including water, liquid nitrogen, graphite, and magnesium.

To support this analysis Monte Carlo simulations have been used to model our experimental approach and to predict the measured results.

2 Experimental Approach

Experiments for this project were carried out in INL's Active Neutron Interrogation Laboratory within a large 9.9 m × 7.6 m test cell which has a concrete floor and concrete walls.[25] The construction of this facility is designed to provide radiation shielding for laboratory workers and the public but it is not specifically designed for high-resolution neutron spectrometry; the high degree of neutron scattering from the floor and walls is evident in the data shown below. The neutron source was placed near the center of the room, 1.48-m above the floor. The neutron spectrometer was placed 0.5-m away from and parallel to the source, parallel to the floor, supported by empty cardboard boxes so it's centerline was 1.48-m above the floor; neutrons from the source were incident on to the side of the detector. Data acquisition equipment was placed on a nearby table and then accessed remotely via computer in order to minimize variations to the scattering environment during the experiments.

2.1 Neutron Source

Initial testing was performed using a deuterium-deuterium (DD) electronic neutron generator (ENG) to produce a monoenergetic neutron field; measurements of the yield of the generator using the indium-foil activation technique have shown it produces approximately $(2.4 \pm 0.6) \times 10^6$ neutrons per second.[26] The ENG was supported above the floor using thin-walled aluminum legs; cylindrical in shape, the ENG axis was perpendicular to the floor with it's target plane at the 1.48-m elevation. Spectral data collected by the spectrometer of the ENG output was used to generate the processing algorithm for pulse rejection; this measurement took 1.52 hours. Following this measurement the neutron generator was replaced with a ^{252}Cf spontaneous fission neutron source (6.43 μg, 3.44 mCi, 0.127 GBq, 1.49×10^7 neutrons per second).[27] The californium source used for these tests is alloyed with a noble metal in the form of a small wire, which is secured within two nested, stainless-steel cylinders. The outer stainless-steel cylinder is 3.25×10^{-2}-m in length and has an outside diameter of 9.4×10^{-3} m; the total steel-wall thickness, both inner and outer capsules, is 2.5×10^{-3} m. The source was taped to the fingers of a steel laboratory vial holder, oriented parallel to the floor with its axis also parallel to the spectrometer. Data was collected

to measure the unaltered neutron spectrum from this source (including room scattering) for 50.5 hours. Data was then taken to measure the neutron spectrum transmitted through different shield objects.

2.2 Attenuating Materials

Four different attenuators were used in these experiments. The attenuators were placed next to the californium source and kept in place using the fingers of a steel laboratory vial holder; a thin cardboard tube was placed underneath heavy objects when needed. The following attenuators were used.

- Water, contained within a thin-walled 236-mL (8-ounce) plastic bottle. The bottle's outside diameter was 6.35×10^{-2} m and its length was 1.32×10^{-1} m. The bottle axis was perpendicular to the ground. The water transmission data reported here was collected over a 91.7-hour period.
- Liquid nitrogen, contained within a glass insulation Dewar. The inside diameter of the Dewar was 6.86×10^{-2} m and it was 2.98×10^{-1} m deep. The Dewar was elevated so that the bottom of the liquid nitrogen column was 3.24×10^{-2} m below the ^{252}Cf source. Data collection was started early one morning and the Dewar was regularly topped-off throughout the day. In the evening the Dewar was filled to the top and then left alone through the night; the next morning there was no longer any liquid nitrogen in the Dewar. The overnight date from the detector was analyzed and a clear transition was observed between when the Dewar was full and when it was empty, this allowed the data to be culled to only include time when the Dewar sufficiently full to have a steady-state neutron count rate. The liquid nitrogen transmission data reported here was collected over a 20.4-hour period.
- Graphite, in the form of a brick measuring 5.08×10^{-2} m wide by 1.02×10^{-1} m tall, the transmission thickness was 6.60×10^{-2} m. The brick was positioned so that the 1.02×10^{-1} m × 5.08×10^{-2} m face was centered on the ^{252}Cf source. The graphite transmission data reported here was collected over a 95.2-hour period.
- Magnesium, in a rectangular form measuring 7.82×10^{-2} m wide by 2.54×10^{-2} m tall, the transmission thickness was 1.93×10^{-2} m. The Mg was positioned so that the ^{252}Cf source was one-third of the distance from the end, centered half-way up the 2.54×10^{-2} m tall block of Mg. The Mg transmission data reported here was collected over a 27-hour period.

2.3 Detector

The detector used for these experiments was the FNS-100 Fast Neutron Spectrometer, a commercial instrument made by made by Bubble Technologies, Inc. (Ontario, Canada). The detector is functionally equivalent to the FNS-100 previously manufactured by Seforad-Applied Radiation Ltd. (Emek Hayaeden, Israel), a gridded ionization chamber that was used in much of the literature cited above. Some general information on this instrument was provided by the vendor to support the modeling effort described below. However, some critically important details of its construction were not available, including the internal dimensions of its construction and the specific composition of internal neutron absorbers. To address some of these deficiencies high-resolution x-ray images were taken to learn the exact location of the ionization chamber within the instrument. Strong reliance was also placed on prior reports by Sailor and Prussin, Evans and Brandenberger, and Fisher et al., which provide an excellent overview of the layout and operating principles of the FNS-100 detector.[4,10,19] An Ortec Model 456 power supply was used to bias the detector.

2.4 Data Acquisition and Processing

Data was collected for these experiments using an Acqiris DC282 high-speed waveform digitizer and stored on high-capacity portable hard drives for post processing. A schematic showing the simple data acquisition equipment set-up used is shown in Figure 1. Post processing was carried out on a computer using algorithms developed using National Instrument's LabView programming language. In essence, the algorithm used for this work was similar to the discrimination techniques implemented previously using analog components; it worked by analyzing the rise time of the waveforms from the ^{3}He ionization chamber and separating longer rise-time events from shorter rise-time events. However, taking advantage of the full capabilities for complete waveform analysis using dPSA, improvements to this simple approach were developed which included the application of additional filters including methods to remove noise and to discriminate pile-up events in the waveform data. Examples of some waveforms that passed the processing algorithm as 'good' events are shown in Figure 2; note that these events have been scaled to have approximately the same magnitude, demonstrating the significant differences in the shapes of these pulses. These waveforms are similar to data of C-S spectrometers reported elsewhere.[11,12]

[Figure 1]

[Figure 2]

3 Modeling

Simulations were developed to model the experiments described here using the MCNP5 radiation transport code.[28] Relatively simple models were initially explored using a Watt-spectrum point source to represent the ^{252}Cf and a cylinder of ^{3}He and methane to represent the sensitive volume of the spectrometer. However, it was quickly apparent that a higher-fidelity representation would be needed in order to accurately predict the high-resolution neutron spectra capable of being generated in the experiments. Previous researchers have commented on the important role high-energy neutron scattering plays in disturbing the spectrum of fast fission neutron fields.[29] Recognizing this, further models were developed that used a previously created representation of the building – including the floor, walls, and ceiling structures, and that included more detailed representations of the californium source, the source support stand, and the attenuator supporting stand.[25] More detail was also included to represent the internal structures of the neutron spectrometer. The simulation results were tallied to determine the volume-averaged neutron spectrum within the sensitive region of the spectrometer, in 10-keV intervals. Neutron capture events were also tallied in the spectrometer's ^{3}He gas, in 10-keV increments as a function of the energy of the neutron leading to the capture events. This information was then used to generate a simulated response function for the spectrometer.

4 Results and Discussion

The first step in these experiments was to collect the data from the DD ENG and to generate the processing algorithm for pulse rejection and acceptance, these results are shown in Figure 3. Measuring the epithermal peak in this spectrum the energy resolution for the spectrometer with the data acquisition set-up used was 34 keV. Prior work has demonstrated that C-S type detectors are capable of achieving epithermal peak resolutions of better than 20 keV. The explanation for the poorer resolution achieved in this work is likely due to the 10-bit resolution of the waveform digitizer, a 12-bit resolution would have been more appropriate. The algorithm discriminates incoming waveforms into three categories. If the rise time of a pulse is not long enough it is identified as a recoil event and

rejected; if a pulse demonstrates too-sharp of deviation in its rise time it is identified as a pile-up or wall-capture event and it is also rejected. Pulses not rejected for these criteria are kept and used for spectrum reconstruction. For the DD neutron data shown here the processing algorithm kept 43% of the full-energy pulses while rejecting 57%. Again, it is likely that a higher precision instrument could be used to improve this performance. The algorithm developed for this project demonstrated a greater level of discrimination then shown in prior work, especially in its ability to eliminate lower-energy recoil events, but this also served to reduce the full energy peak acceptance rate.[19,20,31] The absolute efficiency for C-S type spectrometers, without pulse shape discrimination, has been reported to be $(1.7 \pm 0.5) \times 10^{-4}$ at 2.45 MeV.[19] With the implementation of pulse shape discrimination prior work with analog pulse analysis circuitry has been shown capable of achieving up to 60% acceptance for 6.3-MeV neutrons and up to 80% acceptance for 8.1-MeV neutrons.[1] Knowing that the ENG was operated with an accelerating voltage of 90 keV and that the accelerated ion beam was mostly diatomic, we estimate that the energy of these neutrons was approximately 2.47 MeV.[30] Analysis of the DD neutron spectrum was used to determine an absolute starting-point energy calibration for the system, using the epithermal peak (at 0.764 MeV) and the center of the DD neutron peak. This calibration was later fine-tuned by comparing resonance attenuation features in the attenuation data.

[Figure 3]

Without multienergy, monoenergetic reference neutron spectra it was not possible to determine an absolute efficiency for the system. Instead a comparison was made between the neutron spectrum generated from the processing algorithm for the unattenuated ^{252}Cf source and simulations of the measurement; a scaling function was developed to relate the measured spectrum to the simulated spectrum. The result of this scaling is shown in Figure 4 together with the scaling function. The scaling function shown here is comparable to previously derived efficiency curves.[14,16,17,16,31] It is also similar to previously modeled efficiency estimates for the C-S spectrometer.[32]

[Figure 4]

The efficiency scaling function was then used to adjust the remaining measured neutron spectra to the simulated spectra, the results of this are shown in Figure 5 through Figure 8. These figures also include the total neutron attenuation cross-sections for the primary isotope in each of the attenuating materials. Generally good agreement is seen in the data-simulation comparisons. For the neutron transmission measurement through water agreement exists between the observed and simulated resonance features at 0.44 MeV, 1.00 MeV, and higher energies. The impact of the spectrometer's 37-keV resolution can be easily seen in comparison with the simulation's 10-keV resolution. A small bias appears between the measured and observed neutron spectrum below about 0.75 MeV. For the liquid nitrogen measurement a good level of conformity is observed over the entire energy range including the resonance peak at 0.43 MeV. In this case no lower-energy discrepancy exists between the measured and simulated results. For the graphite measurement the resonance features at 2.08 MeV and in the 2.8 MeV to 3.0 MeV region align well with the simulations although the impact of the spectrometer's lower resolution with respect to the simulation is again clearly seen. In this case a noteworthy discrepancy is seen between the measured and simulated spectra in the 3.2 MeV to 4.5 MeV range, with the scaled, measured results exceeding the simulated spectrum by up to 20%. A low energy discrepancy is seen in this comparison as well. Good overall agreement is evident in the magnesium measurement-simulation comparison including the impact of the 0.26-MeV resonance and the complex higher-energy resonance structure.

[Figure 5]

[Figure 6]

[Figure 7]

[Figure 8]

5 Summary

Digital pulse shape analysis has been used to analyze the rise time of charge pulses from a ^{3}He ionization chamber. This information has been used to separate full-energy neutron capture event signals from nuclear recoil signals and to generate fast neutron histogram plots for a DD ENG, a ^{252}Cf spontaneous fission neutron source, and for the transmitted neutron spectra of ^{252}Cf neutrons through water, liquid nitrogen graphite, and magnesium.

Simulations have been performed to model the response of the ^{3}He spectrometer for the californium measurements and the high-energy resolution of the spectrometer has been demonstrated by examining the effects of neutron resonance absorption in the attenuating materials. Some discrepancies have been identified between the simulations and the measurements, including a slight difference in the low energy region less than 0.75 MeV for the water and graphite, and to a lesser extent for the magnesium transmission measurements. A notable discrepancy between simulation and measurement was also observed for the graphite transmission experiments in the 3.2 to 4.5 MeV range. Further work will be needed to fully understand these differences.

Fast-neutron spectrometry may be used as a complimentary analytical method to support nuclear nonproliferation and nuclear safeguard measurements. For example, accurate determination of the high-energy neutron spectrum from an unknown neutron source can be used to identify the target material in alpha-particle based radioisotope neutron sources. Different low-Z materials produce different characteristic neutron spectra upon alpha-particle irradiation, with different overall energy ranges and very specific energy spectra, and neutron spectrometry may be used to distinguish between these target materials.[33] In some cases neutron spectrometry may be used to identify the alpha-emitting radioisotope; for example, different actinides emit different energy alpha particles and in beryllium there is a neutron spectrum dependence on the energy of the incident alpha particles.[34] Neutron spectrometry may also be capable of providing forensic-level evidence concerning the mean particle size of the subcomponents in $^{9}Be(\alpha,n)$ type neutron sources.[35,36] For safeguards applications fast-neutron spectrometry has the potential to be used as a tool for discriminating between metallic and oxide forms of plutonium, as either a direct method or a supporting method in conjunction with gamma-ray spectrometry.[37,38] Recognizing the impact of the attenuation data for the nitrogen and carbon measurements, neutron spectrometry may also have application in the field of nuclear treaty verification and transparency with a capability to identify the presence of nitrogen-bearing hydrocarbon attenuating materials near neutron sources.

Neutron spectrometry has traditionally been performed using time-of-flight methods using accelerator-based pulsed-neutron sources or nuclear reactors with chopper wheels. However, with the successive closure of many facilities suited for these studies there has been a steady decrease in the on-campus study of neutron spectrometry in education. Recognizing that the experimental infrastructure needed to perform fast neutron spectrometry as outlined in this paper is relatively modest, at least in comparison with other approaches, it seems reasonable to suggest that similar work might provide a good basis for the training of nuclear engineers and

physicists interested in low-energy nuclear physics. Opportunities exist to combine theoretical studies, simulation and modeling, and experimentation within manageable projects that would be suitable for advanced undergraduates and graduate student research. Further, there may be value for systematic, quantitative studies of fast neutron interaction cross sections to reevaluate and perhaps improve the quality of nuclear reference data for neutron scattering in the 0.1 MeV to 6 MeV energy range.

Acknowledgement

This work was supported by Idaho National Laboratory as part of a Laboratory Directed Research and Development funded project. Idaho National Laboratory is operated for the U.S. Department of Energy by Battelle Energy Alliance under DOE contract DE-AC07-05-ID14517.

References

[1] A. Sayres, M. Coppola, Rev. Sci. Instr. 35 (4) (1964) 431-437.
[2] J. M. Cuttler, S. Shalev, Y. Dagan, Trans. Amer. Nucl. Soc. 12 (1) (1969) 63.
[3] J. M. Cuttler, S. Greenberger, S. Shalev, Nucl. Instr. Meth. 75 (1969) 309-311.
[4] W. C. Sailor, S. G. Prussin, Nucl. Instr. Meth. 173 (1980) 511-515.
[5] A. E. Evans, Rad. Effects 96 (1-4) (1986) 1-4.
[6] Moler, R. B., A Fast-Neutron Spectrometer of Advanced Design, Final Report for the National Aeronautics and Space Administration, IIT Research Institute, Chicago, Ill. (1966).
[7] J. W. Marsh, D. J. Thomas, M. Burke, Nucl. Inst. Meth. A 366 (1995) 340-348.
[8] M. Manalopoulou, M. Fragopoulou, S. Stoulos, C. Koukarava, A. Spyrou, G. Perdikakis, S. R. Hashemi-Nezhad, M. Zamani, Nucl. Instr. Meth. A 562 (2006) 371-379.
[9] A. R. Sayres, K. W. Jones, C. S. Wu, Phys. Rev. 122 (6) (1961) 1853-1863.
[10] A. E. Evans, J. D. Brandenberger, High Resolution Fast Neutron Spectrometry Without Time-of-Flight, Report No. LS-UR-78-2562, Los Alamos Scientific Laboratory, Los Alamos, N.M. (1978).
[11] E. Dietz, M. Matzke, W. Sosaat, G. Urbach, M. Weyrauch, Nucl. Instr. Meth. A 332 (1993) 521-528.
[12] N. Takeda, K. Kudo, IEEE Trans. Nucl. Sci. 42 (4) (1995) 548-551.
[13] H. Takahashi, J. Kawarabayashi, T. Kurahashi, T. Iguchi, M. Nakazawa, Nucl. Instr. Meth. A 353 (1994) 164-167.
[14] S. Shalev, J. M. Cuttler, Nucl. Sci. Eng. 51 (1973) 52-66.
[15] H. Ohm, W. Rudolph, K.-L. Kratz, Nucl. Phys. A 274 (1976) 45-52.
[16] H. Franz, W. Rudolph, H. Ohm, K.-L. Kratz, G. Herrmann, F. M. Nuh, D. R. Slaughter, S. G. Prussin, Nucl. Instr. Meth. 144 (1977) 253-261.
[17] H. Ohm, K.-L. Kratz, S. G. Prussin, Nucl. Instr. Meth. A 256 (1987) 76-90.
[18] A. Sayres, Trans. Amer. Nucl. Soc. 7 (2) (1964) 372-373.
[19] W. A. Fisher, S. H. Chen, D. Gwinn, R. R. Parker, Nucl. Instr. Meth. 219 (1984) 179-191.
[20] A. E. Evans, Trans. Amer. Nucl. Sci. 38 (1981) 582-584.
[21] J. G. Owen, D. R. Weaver, J. Walker, Nucl. Instr. Meth. 188 (1981) 579-593.
[22] D. R. Weaver, J. G. Owen, J. Walker, Nucl. Instr. Meth. 198 (1982) 599-602.
[23] T. Cousins, The Employment of a ^{3}He-Based Fast Neutron Spectrometer to Augment the DREO Radiation Measurement System, Report No. 935, Defence Research Establishment Ottawa, Ottawa, Canada (1985).
[24] P. P. Gokhale, E. M. A. Hussein, App. Rad. Isot. 48 (7) (1997) 973-979.
[25] D. L. Chichester, E. H. Seabury, J. M. Zabriskie, J. Wharton, A. J. Caffrey, App. Rad. Isot. 67 (2009) 1013-1022.

[26] C. L. Ruiz, R. J. Leeper, F. A. Schmidlapp, G. Cooper, D. J. Malbrough, Rev. Sci. Instr. 63 (10) 1992) 4889-4891.
[27] R. C. Martin, J. B. Knauer, P. A. Balo, App. Rad. Iso. (2000) 785-792.
[28] MCNP: A General Monte Carlo N-Particle Transport Code, Version 5, Report LA-CP-03-0245, Los Alamos National Laboratory, Los Alamos, N.M. (2003).
[29] A. E. Evans, IEEE Trans. Nucl. Sci. NS-32 (1) (1985) 54-59.
[30] J. Csikai, Handbook of Fast Neutron Generators, CRC Press Inc, Bocas Raton, Fla. (1987).
[31] A. E. Evans, L. V. East, Evaluation of a Gridded ^{3}He Spectrometer Tube for Safeguards and Other Nuclear Applications, in: Nuclear Analysis research and Development Program Status Report January – April 1973, Report No. LA-5291-PR, LS-UR-78-2562, Los Alamos Scientific Laboratory, Los Alamos, N.M. (1973) 17-19.
[32] W. C. Sailor, S. G. Prussin, M. S. Derzon, Nucl. Instr. Meth. A 270 (1988) 527-536.
[33] Neutron Sources for basic Physics and Applications, vol. 2, S. Cierjacks, ed., Pergamon Press, Elmsford, N.Y. (1983)
[34] K. W. Geiger, L. Van Der Zwan, Nucl. Instr. Meth. 131 (1975) 315-321.
[35] L. Van Der Zwan, Can. J. Phys. 46 (1968) 1527-1536.
[36] J. Chen, P. Zhu, Y. Li, Z. Liu, G. Zhang, Nucl. Instr. Meth. A 583 (2007) 407-411.
[37] J. L. Dolan, M. Flaska, S. A. Pozzi, D. L. Chichester, J. Nucl. Mat. Manag. 38 (2009) 40.
[38] D. J. Mercer, et al., Discrimination Between PuO_2 and Pu Metal by Gamma-Ray Spectroscopy, Report LA-UR-01-4870, Los Alamos National Laboratory, Los Alamos, N.M. (2001).

FIGURES AND CAPTIONS

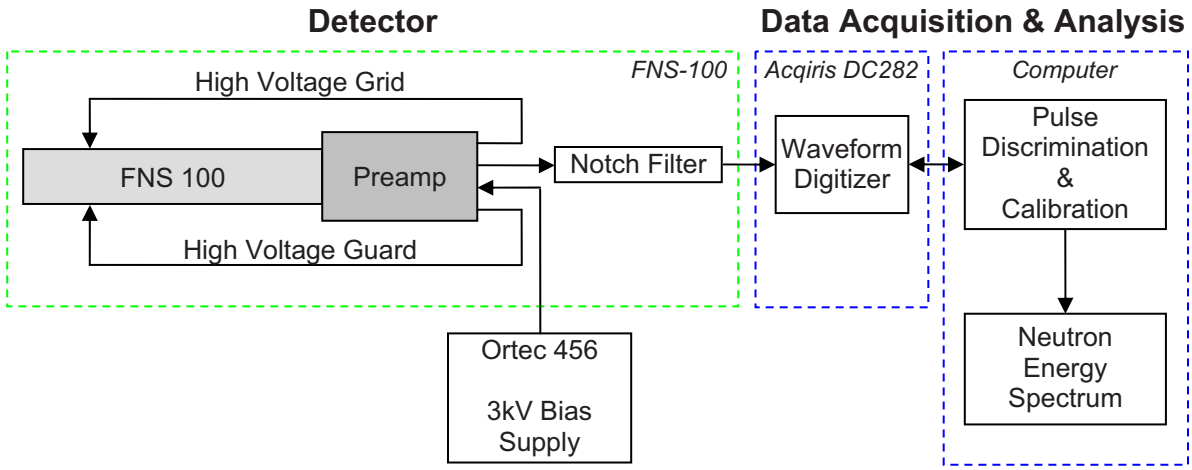

Figure 1 Schematic layout of the electronic data acquisition setup used for this work.

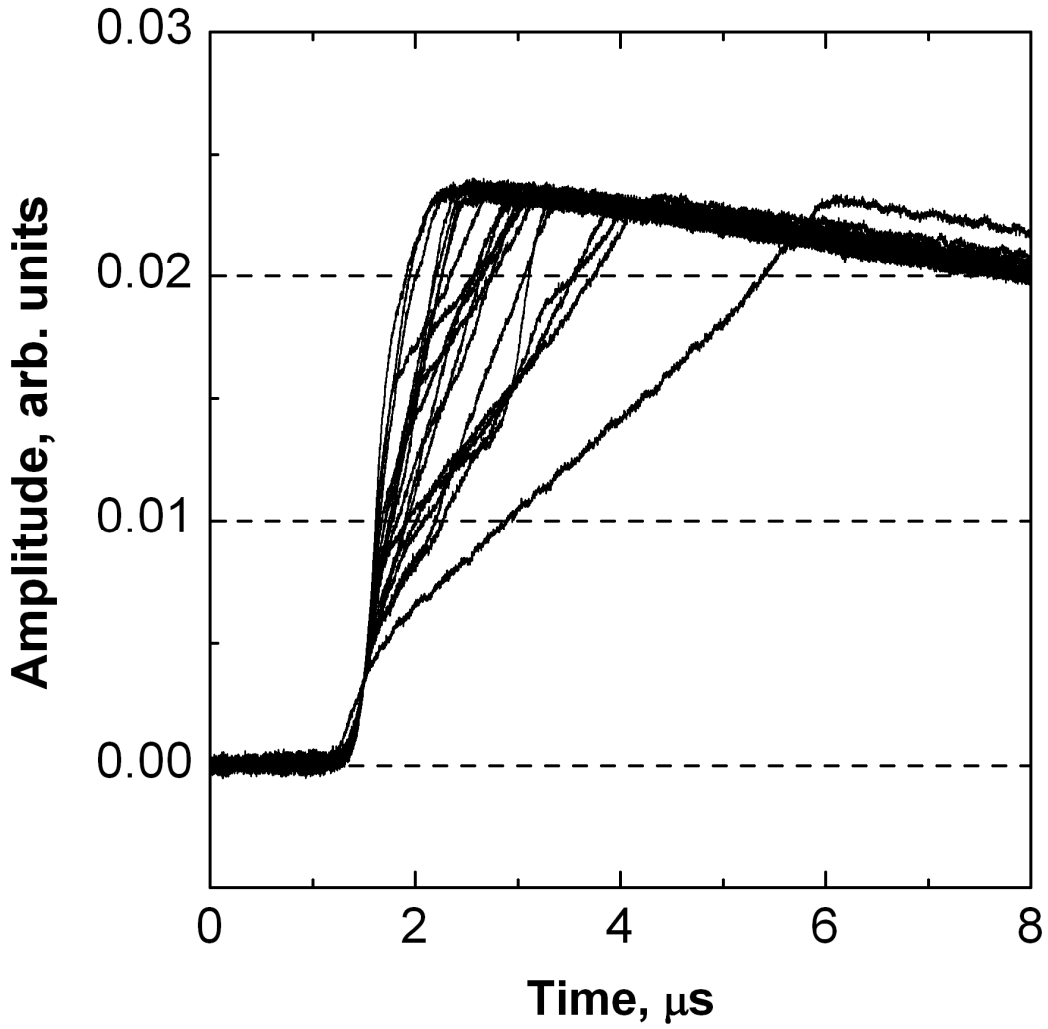

Figure 2 Examples of valid neutron capture event waveforms (data has been scaled).

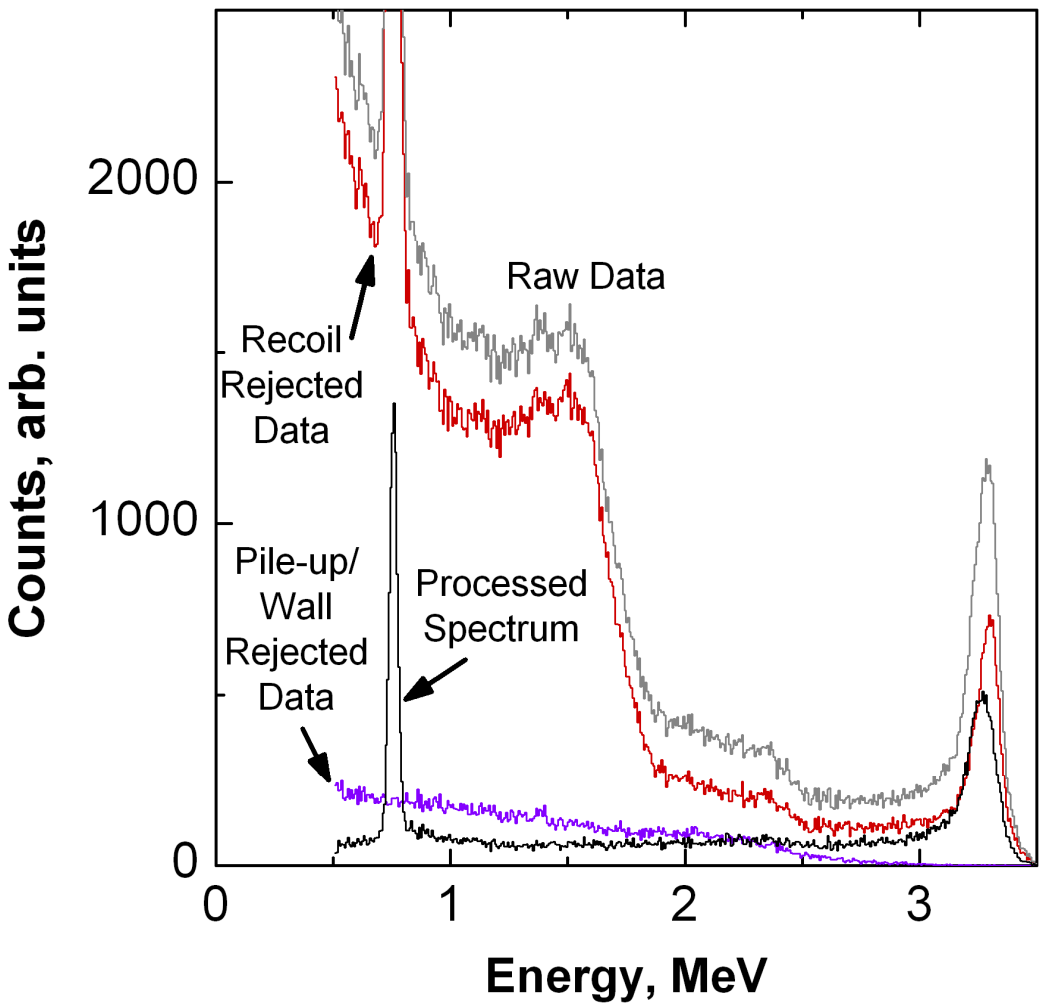

Figure 3 This figure shows the raw data from the spectrometer (gray) from exposure to the DD ENG together with the processing algorithm's rejected data for recoil events (rise time too short, red) and pile-up and wall-interaction events (waveform too distorted, purple). Also shown here is the remaining 'valid' spectral data (black) after the recoil and pile-up events have been subtracted from the raw data.

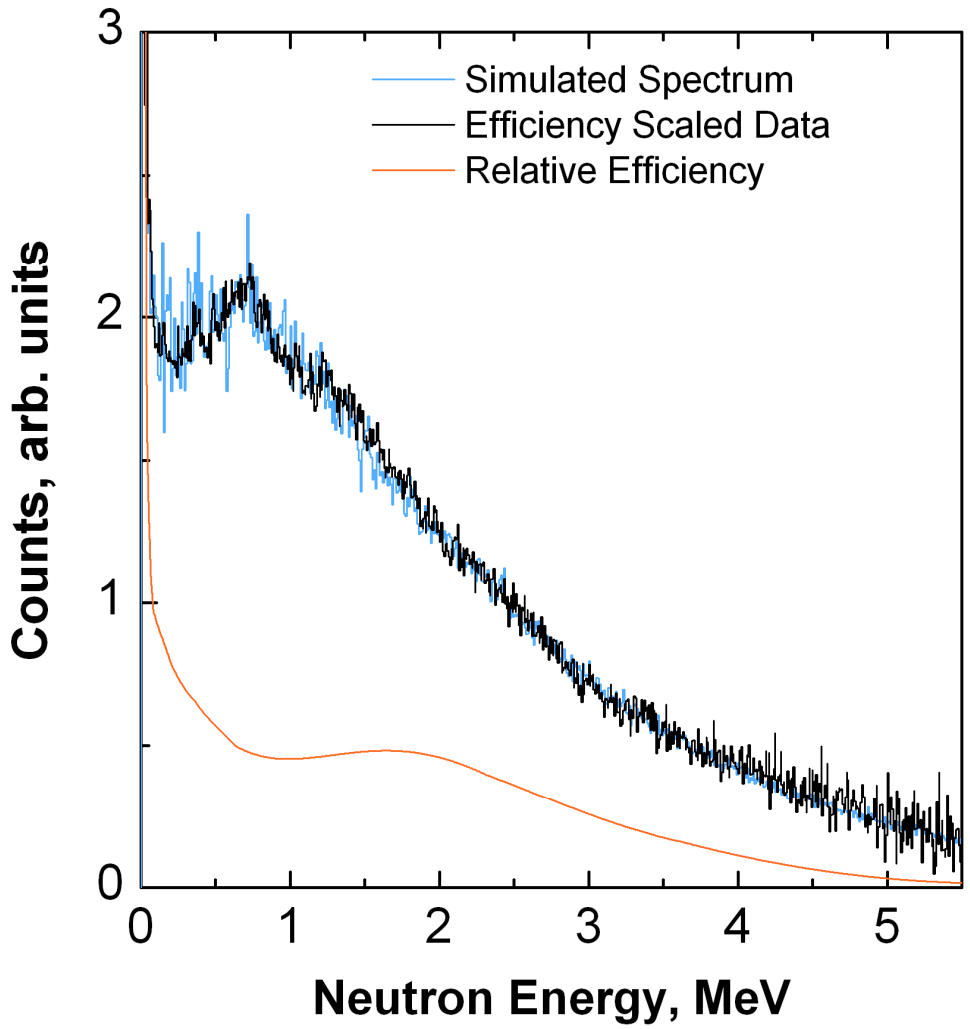

Figure 4 The simulated ^{252}Cf neutron spectrum (Watt fission distribution, blue), the measured data scaled to match the simulated spectrum (black), and the scaling function (orange).

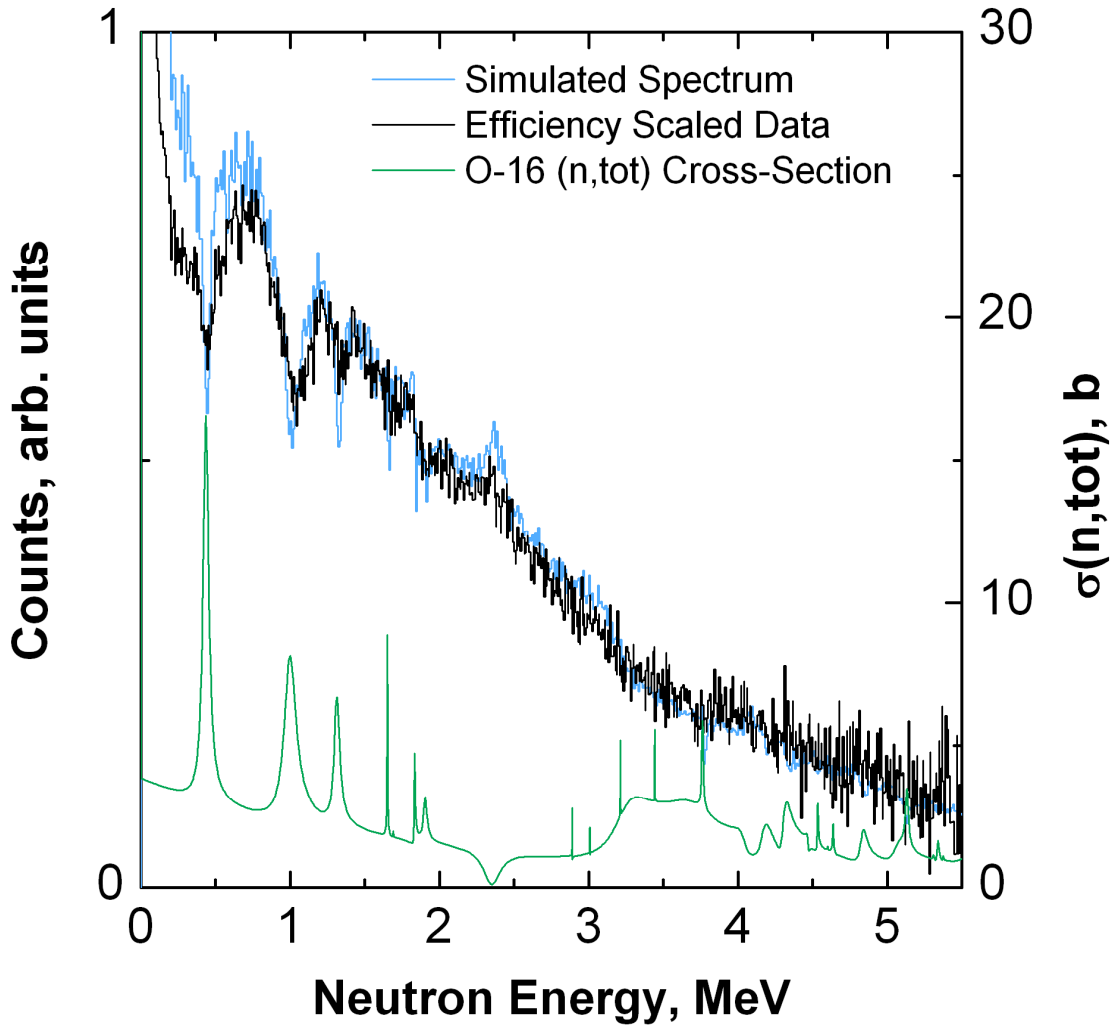

Figure 5 The simulated and efficiency-scaled neutron transmission spectrum for water, together with the total neutron attenuation cross section for ^{16}O.

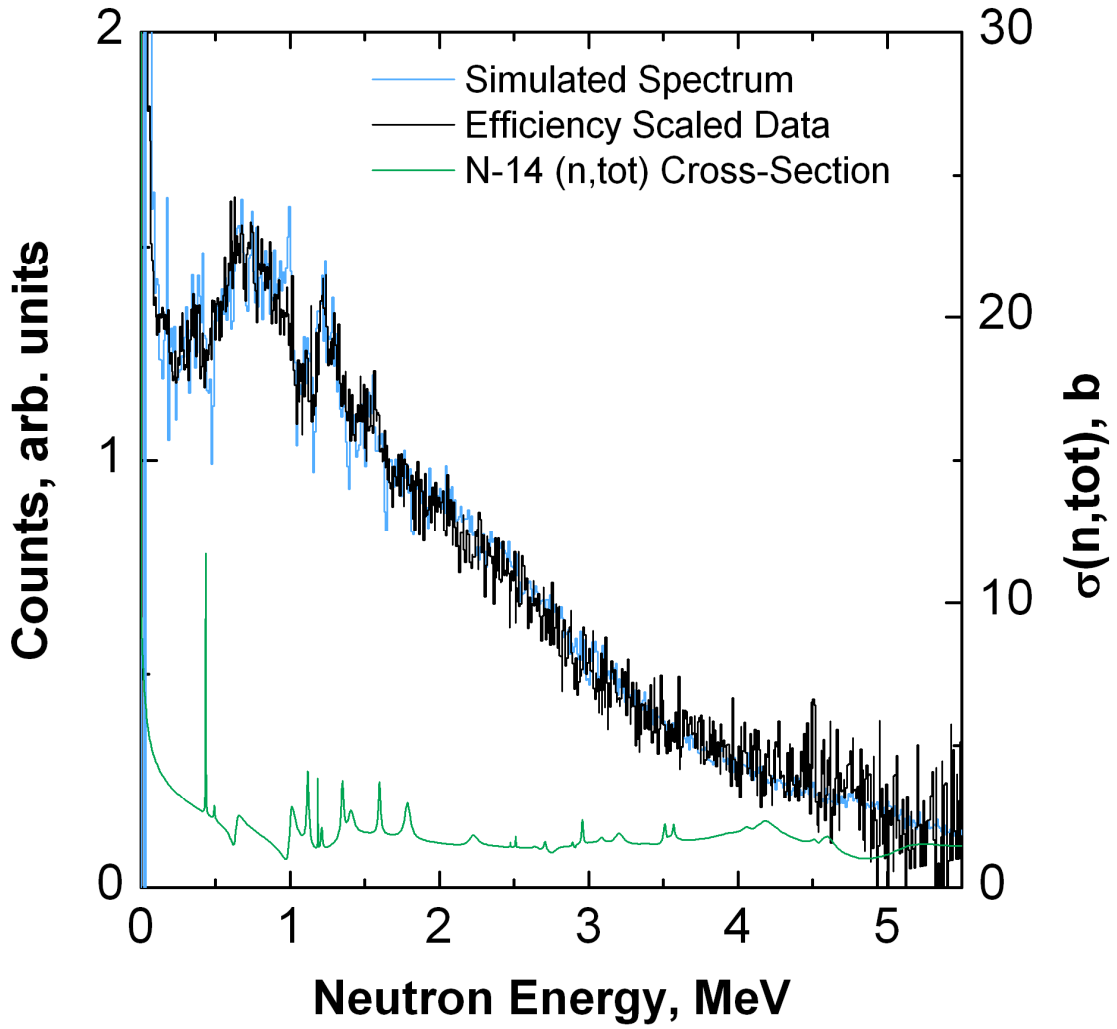

Figure 6 The simulated and efficiency-scaled neutron transmission spectrum for liquid nitrogen, together with the total neutron attenuation cross section for ^{14}N.

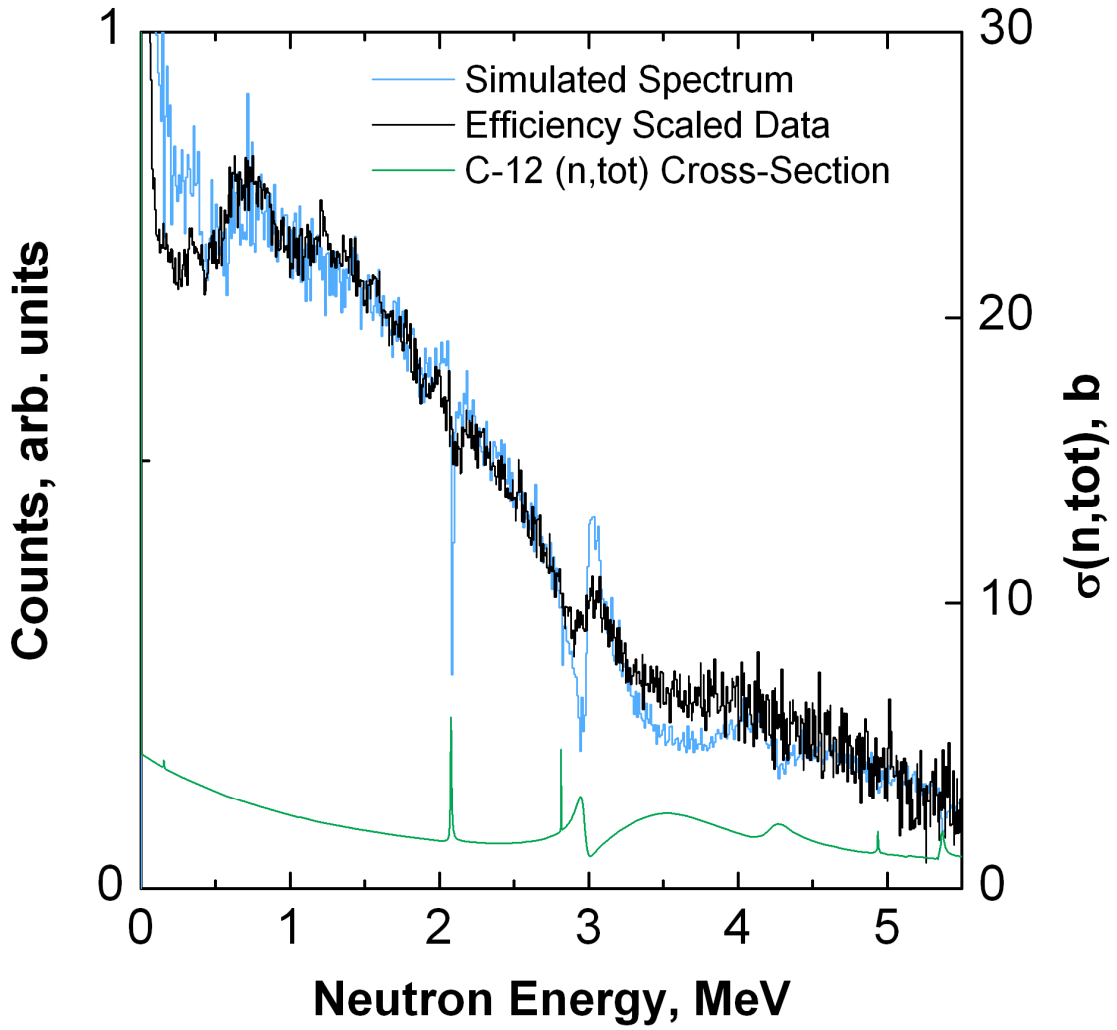

Figure 7 The simulated and efficiency-scaled neutron transmission spectrum for graphite, together with the total neutron attenuation cross section for ^{12}C.

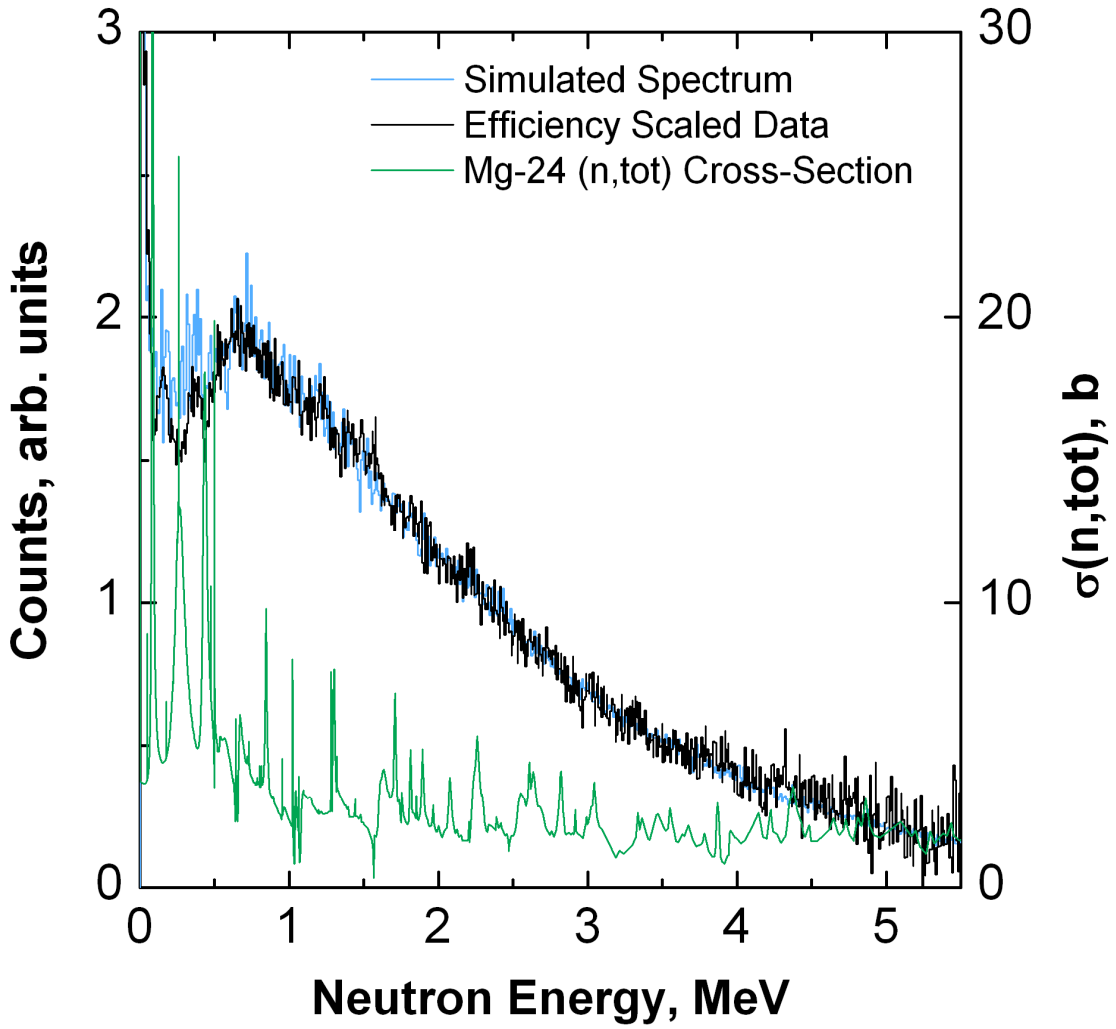

Figure 8 The simulated and efficiency-scaled neutron transmission spectrum for magnesium, together with the total neutron attenuation cross section for ^{24}Mg.